Current Biology *16*, 1428–1434, July 25, 2006 ©2006 Elsevier Ltd All rights reserved DOI 10.1016/j.cub.2006.05.056

Report

How *Much* the Eye Tells the Brain

Kristin Koch,[1] Judith McLean,[1] Ronen Segev,[2] Michael A. Freed,[1] Michael J. Berry II,[2] Vijay Balasubramanian,[3] and Peter Sterling[1,*]
[1] Department of Neuroscience
University of Pennsylvania
Philadelphia, Pennsylvania 19104
[2] Department of Molecular Biology
Princeton University
Princeton, New Jersey 08544
[3] Department of Physics
University of Pennsylvania
Philadelphia, Pennsylvania 19104

Summary

In the classic "What the frog's eye tells the frog's brain," Lettvin and colleagues [1] showed that different types of retinal ganglion cell send specific kinds of information. For example, one type responds best to a dark, convex form moving centripetally (a fly). Here we consider a complementary question: how *much* information does the retina send and how is it apportioned among different cell types? Recording from guinea pig retina on a multi-electrode array and presenting various types of motion in natural scenes, we measured information rates for seven types of ganglion cell. Mean rates varied across cell types (6–13 bits · s^{-1}) more than across stimuli. Sluggish cells transmitted information at lower rates than brisk cells, but because of trade-offs between noise and temporal correlation, all types had the same coding efficiency. Calculating the proportions of each cell type from receptive field size and coverage factor, we conclude (assuming independence) that the approximately 10^5 ganglion cells transmit on the order of 875,000 bits · s^{-1}. Because sluggish cells are equally efficient but more numerous, they account for most of the information. With approximately 10^6 ganglion cells, the human retina would transmit data at roughly the rate of an Ethernet connection.

Results

Natural Stimuli Differed from White Noise

The information rate for a ganglion cell responding to white noise is proportional to the information rate of a Poisson firing neuron with the same mean spike rate [2]. However, white noise is unsuited for calculating *natural* information rates because it contains all frequencies equally, whereas natural images contain spatio-temporal frequencies that are highly skewed (Figure 1) [3–6]. Therefore, we presented the guinea pig retina with video images of natural scenes to mimic the main categories of biological motion: saccades, optic flow, object motion, and fixational eye movement. For these stimuli, the intensity distributions and the spatial and temporal spectra differed strikingly from white noise (Figure 1). Instead, like the distributions typical of natural images, they were skewed toward low intensities and low spatial and temporal frequencies.

Responses Depended on Cell Type

Various cell types were recorded simultaneously on a multi-electrode array [7] or singly with a loose patch electrode [2] and identified by their characteristic reverse correlograms and autocorrelograms (see Figure S1 in the Supplemental Data available with this article online) [8–10]. Comparing responses to a given stimulus across seven cell types, we found a characteristic response pattern for each type (Figure 2). For example, in response to the saccade stimulus, brisk-transient cells (both ON and OFF) fired spike bursts that peaked high in the PSTH (>300 spikes · s^{-1}), whereas brisk-sustained cells (both ON and OFF) peaked lower (~150 spikes · s^{-1}) and fired for longer periods (Figure 2). ON-OFF direction-selective cells fired with low jitter in spike timing across trials, whereas local-edge cells fired with considerable jitter (Figure 2 saccade, standard deviation of spike times across trials was 9 ms versus 43 ms).

On the other hand, while comparing responses across four different stimuli, we found that characteristic response patterns were stable (Figure 2). For example, brisk-transient peaks always exceeded 200 spikes · s^{-1} and ON-OFF direction-selective cells always fired with low jitter in spike timing (Figure 2; 9–17 ms), whereas local-edge cells always fired with considerable jitter (Figure 2; 18–68 ms). We quantified these observations by comparing five basic statistics of the spike train: peak rate, mean rate, temporal jitter (standard deviation of spike timing across repeats [2]), burst fraction (fraction of spikes that occurred <6 ms apart), and firing fraction (fraction of time bins during which a cell fired at $\geq$5% of its peak rate). Spike statistics were constant across stimuli, and this was true for all cell types. Each statistic depended on cell type (two-way analysis of variance, Bonferroni/Dunn post-hoc test, $p < 0.05$), whereas spike statistics generally did not depend on the stimulus ($p > 0.05$). The only exception was that the local-edge cell type fired with significantly greater spike-time jitter to the object motion stimulus than to the fixational stimulus (Figure S2; $p < 0.05$).

Because spike statistics differed between cell types more than between stimuli, the rank ordering of cells was consistent across stimuli and the key response features of each cell type were preserved (Figure S2). Thus, brisk-transient cells always had the largest burst fraction and highest peak rates; brisk-sustained cells usually had the largest firing fraction, and direction-selective cells usually had the smallest firing fraction. Direction-selective and local-edge cells always fired at about half the mean rate of brisk cells; local-edge cells usually had the greatest timing jitter. When pooled

*Correspondence: peter@retina.anatomy.upenn.edu

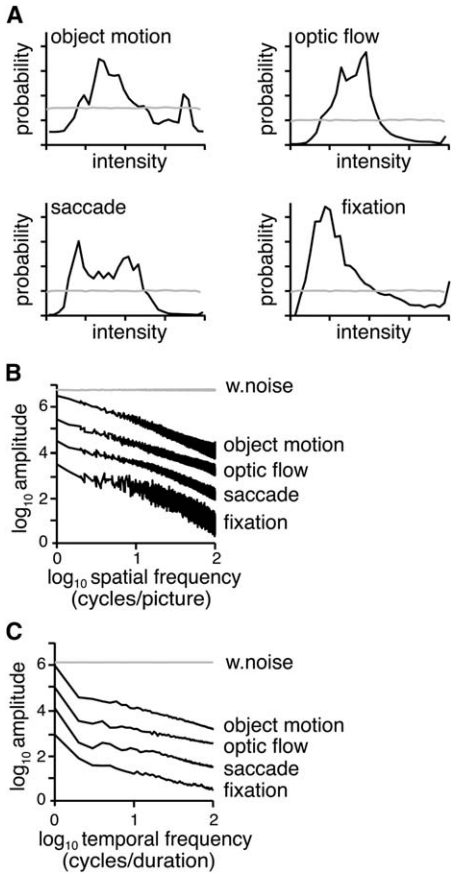

Figure 1. Statistics of Natural Stimuli Differ from Those of White Noise

Natural movies mimicked saccades, optic flow, and object motion [10]. To mimic fixational eye movements, we used Psychophysics toolbox [40, 41] to jitter van Hateren's images (http://hlab.phys.rug.nl/archive.html) randomly over the retina, with step size and velocity matched to that measured for the rabbit [9, 42]. When projected onto the retina, stimuli filled approximately 4 mm × 4 mm with mean luminance corresponding to photopic vision. The photon absorption rates were 2900 and 440 photons · s^{-1} for the M and S cones, respectively. Each movie lasted 20–27 s and was repeated 60–100 times. Intensity distributions and amplitude spectra were obtained after averaging over all frames.

(A) Intensities in white noise (gray lines) are equally represented, but in natural scenes (black lines), lower intensities are more likely.

(B) Spatial frequencies in white noise have equal amplitude, but in natural scenes, amplitude declines with frequency (slope ~ −1.5). Spectra have been separated (shifted up) for clarity.

(C) Temporal frequencies in white noise have equal amplitude, but in natural motion, amplitude declines with frequency (slope ~ −1.0). Spectra have been shifted up for clarity.

across stimuli and compared with a one-way ANOVA, brisk-transient cells had the highest burst fractions and fired at the highest peak rates (Table 1; $p < 0.05$), and ON-OFF direction-selective cells fired at higher peak rates than local-edge cells ($p < 0.05$). Brisk-sustained cells had higher firing fractions than direction-selective cells ($p < 0.05$). Brisk-transient cells fired at the highest mean rates ($p < 0.05$). Local-edge responses to saccades, optic flow, and object motion showed the highest timing jitter ($p < 0.05$). No other significant differences were found in the responses of the different cell types. Because ON and OFF cells of the same class (brisk-transient, brisk-sustained) were similar (Table 1), they were pooled in subsequent analyses.

Information Rate Correlated with Mean Spike Rate

The information rate was moderately correlated with peak spike rate and firing fraction (respectively, $r = 0.57$ and 0.48) but strongly correlated with mean spike rate ($r = 0.90$; Figure 3A). Information rate was negatively correlated with timing jitter ($r = -0.29$) because jitter increases noise entropy. Thus, cell types with the highest mean spike rates and lowest jitter (brisk-transient) sent the most bits · s^{-1} (Figure S2). Information rate depended on cell type ($p < 0.05$) and not on the stimulus ($p > 0.05$). Information rate was constant across stimuli, and this was true for all cell types (Figure S2; $p > 0.05$). Averaged across stimuli, the information rates of brisk-transient cells were highest (Table S1; $p < 0.05$).

Information per Spike Decreased with Mean Spike Rate

The average information per spike (information rate divided by mean spike rate) was highest for the lowest spike rates (~3.5 bits · $spike^{-1}$ vs. ~1 bit · $spike^{-1}$ for the highest rate (Figure 3D)). This agrees with the information-theory principle that rarer events carry more information per event [11–13]. Accordingly, cells with lower mean spike rates (typically ON direction-selective cells, ON-OFF direction-selective cells, and local-edge cells) sent approximately 20% more bits · $spike^{-1}$ than the brisk types (Table S1).

All Cell Types Filled Their Coding Capacities Similarly

Cells with higher spike rates have a greater capacity to encode information, but some cells might make better use of their capacity than others, i.e., might show greater coding efficiency. Coding capacity is the maximum total entropy rate possible at the mean spike rate [2, 11, 14]. It is achieved when spikes are independent (have no temporal correlations) and when the spike train is perfectly reproducible (there is no noise entropy). Coding capacity, C, is calculated as

$$C(R,\Delta t)=\frac{-R\Delta t\log_2(R\Delta t)-(1-R\Delta t)\log_2(1-R\Delta t)}{\Delta t}\text{bits}\cdot\text{s}^{-1} \quad (1)$$

where R = mean spike rate and Δt = 5 ms, i.e., the time bin used to calculate information. Coding efficiency is a cell's actual information rate divided by its coding capacity.

Coding capacity differed across types—with means ranging from ~20 bits · s^{-1} for direction-selective and local-edge cells to ~40 bits · s^{-1} for brisk cells. However, all types showed the same coding efficiencies (~30% of capacity; Figure 3A and Table S1; $p < 0.05$). Coding efficiency was also the same across stimuli, and this was true for all cell types (Figure S2; $p > 0.05$).

What Sets Coding Efficiency?

Total entropy averaged across cells and stimuli filled 91% of capacity (Figure 3B). This implied that 9% was lost to temporal correlations. The fractional loss depended on cell type: brisk-transient cells lost 15%,

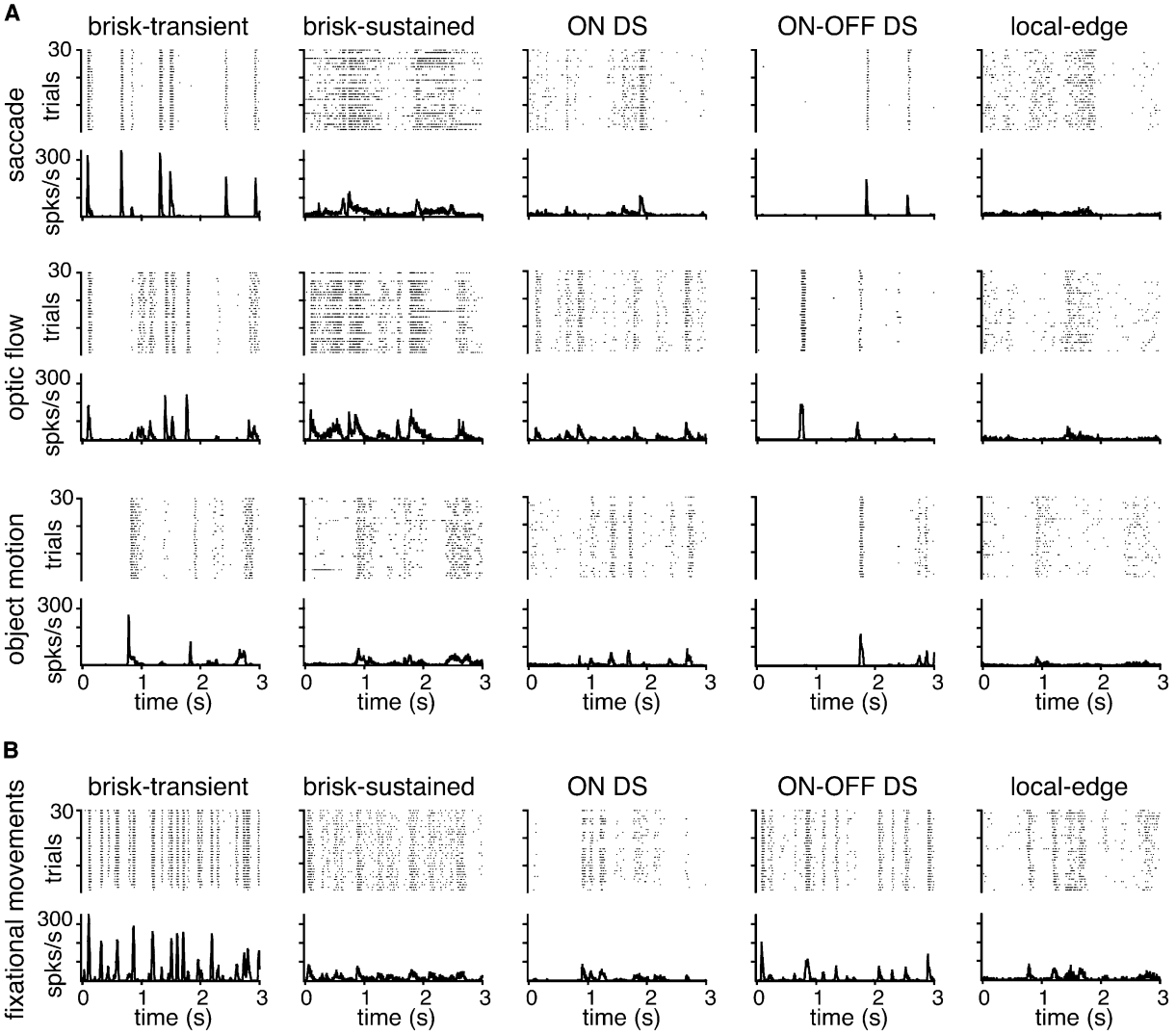

Figure 2. Four Types of Natural Motion Evoked Similar Spike Patterns within a Cell Type But Different Patterns Across Types

(A) All five cells were recorded simultaneously (multi-electrode array). Each cell responded similarly to all three motion stimuli. The brisk-transient and ON-OFF direction-selective (DS) cells responded with high peak rates and low firing fractions, whereas the brisk-sustained, ON DS, and local-edge cells responded with lower peak rates and higher firing fractions. The brisk-transient and ON-OFF DS responses showed the lowest spike-time jitter across trials, whereas the brisk-sustained and local-edge responses showed the highest. As expected for sluggish types, mean firing rates were about half that of the brisk cell types [2].

(B) Cells were recorded singly (loose-patch). Spike patterns to simulated fixational eye movements resembled those of the other types of motion.

whereas local-edge cells lost only 4% (Table S1; $p < 0.05$). Noise entropy averaged across cells and stimuli filled 65% of capacity (Figure 3C). This implies that 65% of capacity was lost to spike train noise. Again, the fractional loss depended on cell type; brisk-transient cells lost 56%, whereas local-edge cells lost 69% ($p < 0.05$). There were no other significant differences across cell types, nor did losses depend on the stimulus ($p > 0.05$). Most cells lost more capacity to spike train noise than to temporal correlations between spikes.

Cell types differing in temporal correlations and noise could transmit with equal efficiency if larger losses due to correlations were offset by smaller losses to noise. This is precisely what we found (Figure 3E; Table S1). For brisk-transient cells, total entropy filled a small fraction of capacity because spikes were strongly correlated, whereas noise entropy was reduced. Conversely, for local-edge cells, total entropy filled a larger fraction of capacity because spikes were weakly correlated, whereas noise entropy was elevated. Thus, coding efficiency was conserved across cell types because losses due to temporal correlations were finely balanced against losses due to noise.

This balance would be achieved if spike bursts (which inevitably produce correlations) also increase reliability. This is precisely what we found. Spike trains with many bursts (high burst fractions) had much less total entropy compared to their capacities than did spike trains with few bursts (Figure 3F). Bursty spike strains also tended toward lower noise entropy (Figure 3G). This occurs partly because the spike rate during a burst approaches the refractory period; inter-spike intervals are thus regularized, and the spike train's variability is reduced [15].

Table 1. Spike Train Statistics Averaged over All Natural Stimuli

Cell Type	Burst Fraction	Peak Spike Rate (Hz)	Firing Fraction	Mean Spike Rate (Hz)	Jitter (ms)
Brisk-transient (n = 41)	0.26 ± 0.12	171 ± 71	0.22 ± 0.18	8 ± 5	15 ± 7
ON brisk-transient (n = 9)	0.27 ± 0.12	157 ± 77	0.33 ± 0.24	10 ± 6	19 ± 10
OFF brisk-transient (n = 32)	0.26 ± 0.12	175 ± 70	0.19 ± 0.14	7 ± 4	14 ± 6
Brisk-sustained (n = 65)	0.10 ± 0.12	104 ± 38	0.29 ± 0.19	6 ± 4	23 ± 9
ON brisk-sustained (n = 27)	0.11 ± 0.12	119 ± 39	0.29 ± 0.23	6 ± 4	20 ± 8
OFF brisk-sustained (n = 38)	0.08 ± 0.12	93 ± 34	0.30 ± 0.19	6 ± 5	26 ± 9
ON DS (n = 15)	0.07 ± 0.12	90 ± 30	0.15 ± 0.11	3 ± 2	18 ± 5
ON-OFF DS (n = 33)	0.08 ± 0.12	117 ± 36	0.17 ± 0.15	4 ± 3	17 ± 7
Local-edge (n = 19)	0.07 ± 0.12	74 ± 36	0.25 ± 0.14	4 ± 3	40 ± 24

Values are given as mean ± SD.

Discussion

Any study employing natural images faces the concern that only a few of all possible images can be tested. Yet, because natural images share statistical regularities (such as scale-invariant power spectra [4] and skewed intensity distributions [16]), our stimuli resembled each other much more than they resembled white noise (Figure 1). Indeed, the information rates measured here are lower than those reported for white noise [2, 17]. This difference probably arises, at least in part, because white noise lacks spatio-temporal correlations.

Another concern, especially for ganglion cells selective for "trigger features," is that particular images might fail to excite certain cell types. Yet, we found that all cells responded to all stimuli over much of their dynamic range. Feature-selective types such as the local-edge cell, considered "sluggish" due to its lower peak and average rates [18], fired up to 75 spikes · s^{-1} and averaged 4 spikes · s^{-1} over the entire recording. This was only 2-fold less than the peak and average responses to artificial stimuli that are deliberately tuned to the trigger features [2]. Far from being silent, the local-edge type showed larger firing fractions than the less selective brisk-transient type (Figure S2). In general, responses differed more across *types* than across stimuli.

How Much Information Does the Eye Send the Brain?

The following calculation treats individual ganglion cells as independent channels. Of course, the messages sent by cells of the same and different types are *not* totally independent. Rather, they are partially correlated and the correlations may be important [10]. To calculate the *net* information conveyed about visual stimuli, one would need to evaluate these correlations. Yet, a calculation that excludes them is still useful because it: (i) allows initial estimates of basic parameters, such as power efficiency (bits · erg^{-1}); (ii) reveals how visual information is distributed among the different neural components; and (iii) provides a sense of scale for thinking about the visual system as a whole.

The guinea pig optic nerve sends about 100,000 axons centrally (our unpublished counts [19, 20]). Brisk-transient ganglion cells (ON + OFF) account for about 6% (Kao and P.S., unpublished data; similar estimates are found in cats [21] and primates [22]). The mean information rate for a single brisk-transient cell is about 13 bits · s^{-1}; thus, the brisk-transient component of the guinea pig optic nerve sends approximately 78,000 bits · s^{-1}. OFF brisk-transient cells are twice as numerous as ON cells in the guinea pig (Borghuis et al., personal communication; see also results for primates [23]). Because OFF and ON transmit at equal rates, the OFF and ON cells contribute, respectively, about 52,000 bits · s^{-1} and 26,000 bits · s^{-1}. This fits the findings that natural contrast distributions are skewed toward negative contrasts [24, 25] and dark regions in natural images contain more information (Ratliff et al., personal communication).

Next we calculated the density for each cell type, from its dendritic-field area and degree of overlap with its neighbors (Table S2). The ratios of cell densities, plus the fact that there are approximately 6,000 brisk-transient cells, yield numbers for the other types studied here: approximately 24,000 brisk-sustained cells, approximately 7,000 ON direction-selective cells, approximately 12,000 ON-OFF direction-selective cells, and approximately 20,000 local-edge cells. This leaves 30% of optic axons to be apportioned among approximately 5 additional cell types [26]. Because these types are all "sluggish" [18], we assigned them the average information rates for additional sluggish cells that were recorded but not classified by type (9 bits · s^{-1}; n = 18). The total information rate for all components in the optic nerve sums to approximately 875,000 bits · s^{-1} (Table S2).

Sluggish Cells Transmit Most Information

Most studies of ganglion-cell coding have focused on the brisk types (X and Y in cats, M and P in primates). The sluggish types, despite their similar S/N ratio [27] and large contribution to the optic nerve [18], have been largely ignored. Thus, it is startling to realize that the famous brisk-transient cells contribute only 9% of the information sent down the optic nerve, whereas the more mysterious local-edge cells contribute nearly twice as much! Overall, the non-brisk types contribute 64% of the information; and thus far outscore the brisk types (Table S2).

Correlations in the messages sent by different cells will affect the net information transmitted about visual stimuli relative to the total information and might also affect the proportion carried by each cell type. However, existing measurements suggest comparable redundancies in the responses of different cell classes, with a significant fraction of the "shared information" arising from receptive-field overlap [10, 28]. Thus, when the correlations are accounted for, the sluggish category will probably carry at least as much information as the brisk category—and substantially more than the brisk-transient types.

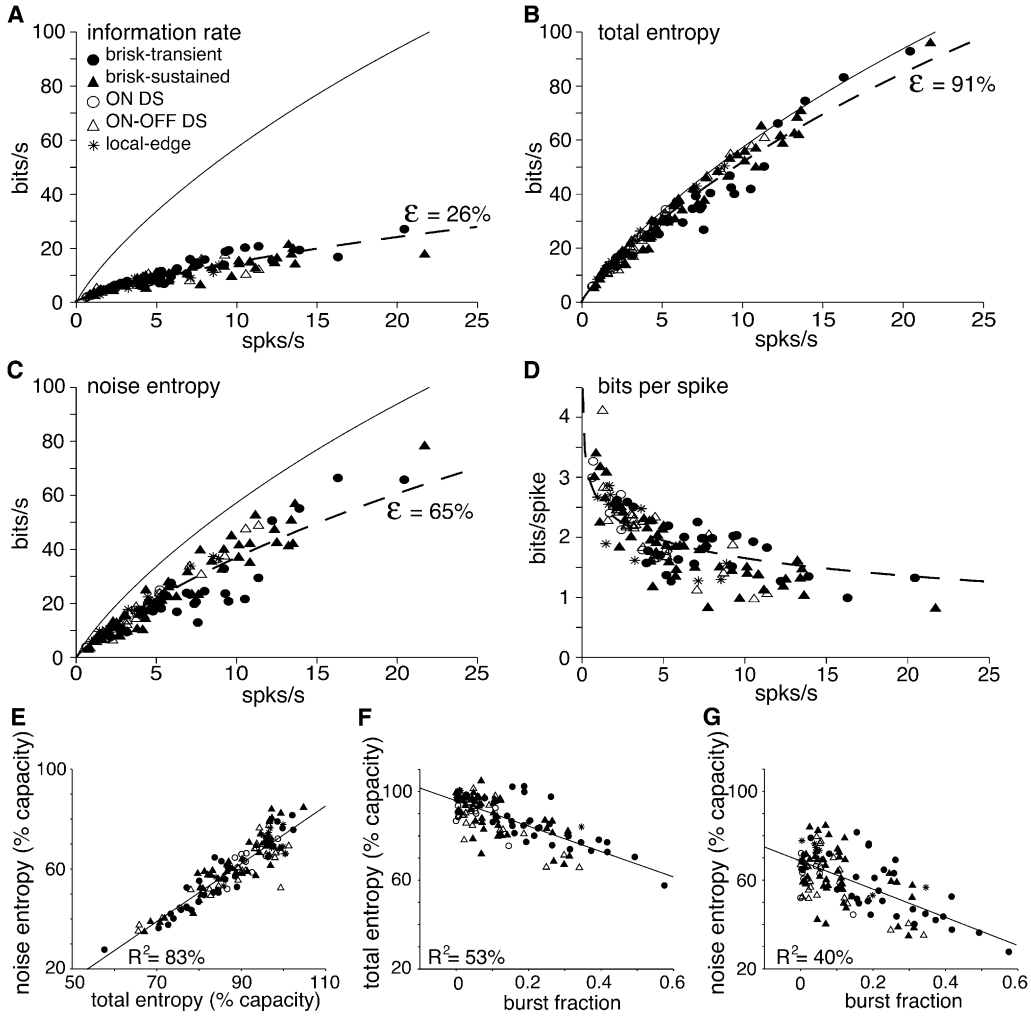

Figure 3. All Cell Types Transmitted Information with Similar Efficiency Because Total Entropy and Noise Entropy were Correlated by Spike Train Bursts

Information rate (total entropy–noise entropy) was estimated by the direct method [43] with bin width (Δt) = 5 ms and spike word-lengths up to eight digits. Bin width was set by the longest refractory period (5 ms for local-edge cells). Estimates of total and noise entropy were extrapolated to infinite data size [44]. Estimated total and noise entropies were within 15% of that calculated for the longest word. A solid line shows the coding capacity of a ganglion cell assuming noiseless firing with no spike correlations ($C(R, \Delta t)$; see text). A dashed line shows the fraction of coding capacity (ε that best fit information rate, total entropy, or noise entropy).

(A) Information rate was 26% of coding capacity (0.26 $C(R,\Delta t)$). K^2 (percent of variation unexplained by coding capacity equation) was 19%.

(B) Total entropy was 91% of coding capacity. K^2 = 4%.

(C) Noise entropy was 65% of coding capacity. K^2 = 12%.

(D) A dashed line indicates the fraction of coding capacity per spike, (0.26 * $C(R,\Delta t)$)/R. Lower rates carry more bits per spike.

(E) Line is least squares fit: slope = 1.2 (R^2 = coefficient of determination). Noise entropy is strongly correlated with total entropy.

(F) Burst fraction is the fraction of spikes with interspike intervals <6 ms. Line is least squares fit: slope = −0.6. Total entropy as a fraction of capacity decreased with burst fraction.

(G) Line is least squares fit; slope = −0.6. Noise entropy as a fraction of capacity decreased with burst fraction.

Why Are There Many Ganglion Cell Types?

Nerve fibers in the frog auditory nerve are reported to encode naturalistic stimuli with an efficiency sometimes reaching approximately 90% of capacity (4-fold greater than for white noise [29]). This differs strikingly from optic fibers, where coding efficiency to naturalistic stimuli is 3-fold worse than in auditory fibers and where there is little (if any) enhancement compared to white noise. Naturally one wonders why an optic fiber fares so poorly in these comparisons. Our tentative answer bears on the question of why the retina uses so many cell types.

Auditory fibers apparently achieve their high coding efficiency via a "tuned" nonlinear filter that selectively amplifies the anticipated signal [29]. A similar strategy is apparently used by the mammalian rod bipolar cell to encode single photon responses [30]. However, this coding strategy, highly effective when the anticipated signal is sparse and well defined, may serve poorly for ganglion cells because the information of biological interest in natural scenes is so varied that highly tuned, nonlinear filters would either reject too much information or require too many cell types.

Given the ganglion cell strategy of broad tuning and equal coding efficiency, why does the retina not send all visual information over one cell type with a high information rate? This is possibly because the energetic cost of signaling increases nonlinearly with temporal frequency and information rate of individual axons [31–34]. To illustrate, we compare the cost of transmitting 300 bits · s^{-1} over a bundle of independent axons with mean spike rates of 4 Hz (local-edge cells), 8 Hz (brisk-transient cells), and 40 Hz (hypothetical high-rate channel). Given approximately 30% efficiency, the 4 Hz neuron sends 2.1 bits · $spike^{-1}$, the 8 Hz neuron sends 1.8 bits · $spike^{-1}$, and the 40 Hz neuron sends only 1.1 bits · $spike^{-1}$ (from Equation 1). Thus, for 300 bits · s^{-1}, the "local-edge" cable would use ~140 spikes · s^{-1}, the "brisk-transient" cable would use ~170 spikes · s^{-1}, and the high-rate cable would use approximately 270 spikes · s^{-1}. Because the dominant metabolic cost in neural signaling is associated with spiking [35, 36], the cables with lower firing rates would save considerable energy. Likewise, theoretical studies predict that metabolic cost is minimized when signals are distributed over many weakly active cells [37].

Of course, there are other reasons to use multiple cell types [38]. Spatial acuity requires narrow-field cells with a high sampling rate [39]. Because such a type must necessarily distribute densely, its information rate should be relatively low to reduce costs. On the other hand, encoding of high stimulus velocities requires extended spatial summation and thus a broad-field cell—plus the ability to transmit at high bit rates so as not to lose the higher temporal frequencies. Such a cell type must necessarily be expensive, but given the extended dendritic field, this type can be sparse. Consequently energetic considerations probably interact with other constraints to set the number of cell types and a general information rate of roughly 10 bits · s^{-1} and 2 bits · $spike^{-1}$.

Supplemental Data

Supplemental Data include two figures and two tables and can be found with this article online at http://www.current-biology.com/cgi/content/full/16/14/1428/DC1/.

Acknowledgments

We thank Nadiya Tkachuk for assisting with the multi-electrode recordings and Charles Ratliff for analyzing the natural stimuli. This work was supported by National Institute of Health grants T32 EY07035, EY08124, EY013333, and EY014196 and National Science Foundation grant IBN0344678.

Received: May 16, 2006
Accepted: May 18, 2006
Published: July 24, 2006

References

1. Lettvin, J.Y., Maturana, H.R., McCulloch, W.S., and Pitts, W.H. (1959). What the frog's eye tells the frog's brain. Proc. Inst. Radio Engr. *47*, 1940–1951.
2. Koch, K., McLean, J., Berry, M., Sterling, P., Balasubramanian, V., and Freed, M.A. (2004). Efficiency of information transmission by retinal ganglion cells. Curr. Biol. *14*, 1523–1530.
3. Dong, D.W., and Attick, J.J. (1995). Statistics of natural time-varying images. Network: Computation in Neural Systems *6*, 345–358.
4. Field, D.J. (1987). Relations between the statistics of natural images and the response properties of cortical cells. J. Opt. Soc. Am. A *4*, 2379–2394.
5. Simoncelli, E.P., and Olshausen, B.A. (2001). Natural image statistics and neural representation. Annu. Rev. Neurosci. *24*, 1193–1216.
6. Eckert, M.P., and Buchsbaum, G. (1993). Efficient coding of natural time varying images in the early visual system. Philos. Trans. R. Soc. Lond. B Biol. Sci. *339*, 385–395.
7. Segev, R., Goodhouse, J., Puchalla, J., and Berry, M.J., 2nd. (2004). Recording spikes from a large fraction of the ganglion cells in a retinal patch. Nat. Neurosci. *7*, 1154–1161.
8. Devries, S.H., and Baylor, D.A. (1997). Mosaic arrangement of ganglion cell receptive fields in rabbit retina. J. Neurophysiol. *78*, 2048–2060.
9. Olveczky, B.P., Baccus, S.A., and Meister, M. (2003). Segregation of object and background motion in the retina. Nature *423*, 401–408.
10. Puchalla, J.L., Schneidman, E., Harris, R.A., and Berry, M.J. (2005). Redundancy in the population code of the retina. Neuron *46*, 493–504.
11. Rieke, F., Warland, D., de Ruyter van Steveninck, R., and Bialek, W. (1997). Spikes: Exploring the Neural Code (Cambridge, MA: MIT Press).
12. Shannon, C.E., and Weaver, W. (1949). The Mathematical Theory of Communication (Urbana, IL: University of Illinois Press).
13. Zador, A. (1998). Impact of synaptic unreliability on the information transmitted by spiking neurons. J. Neurophysiol. *79*, 1219–1229.
14. MacKay, D., and McCulloch, W.S. (1952). The limiting information capacity of a neuronal link. Bull. Math. Biophys. *14*, 127–135.
15. Berry, M.J., 2nd, and Meister, M. (1998). Refractoriness and neural precision. J. Neurosci. *18*, 2200–2211.
16. Richards, W.A. (1982). Lightness scale from image intensity distributions. Appl. Opt. *21*, 2569–2582.
17. Passaglia, C.L., and Troy, J.B. (2004). Information transmission rates of cat retinal ganglion cells. J. Neurophysiol. *91*, 1217–1229.
18. Troy, J.B., and Shou, T. (2002). The receptive fields of cat retinal ganglion cells in physiological and pathological states: Where we are after half a century of research. Prog. Retin. Eye Res. *21*, 263–302.
19. Guy, J., Ellis, E.A., Kelley, K., and Hope, G.M. (1989). Spectra of G ratio, myelin sheath thickness, and axon and fiber diameter in the guinea pig optic nerve. J. Comp. Neurol. *287*, 446–454.
20. Do-Nascimento, J.L., Do-Nascimento, R.S., Damasceno, B.A., and Silveira, L.C. (1991). The neurons of the retinal ganglion cell layer of the guinea pig: Quantitative analysis of their distribution and size. Braz. J. Med. Biol. Res. *24*, 199–214.
21. Wassle, H., Levick, W.R., and Cleland, B.G. (1975). The distribution of the alpha type of ganglion cells in the cat's retina. J. Comp. Neurol. *159*, 419–438.
22. Dacey, D.M. (1994). Physiology, morphology and spatial densities of identified ganglion cell types in primate retina. Ciba Found Symp *184*, 12–28, discussion 28–34, 63–70.
23. Chichilnisky, E.J., and Kalmar, R.S. (2002). Functional asymmetries in ON and OFF ganglion cells of primate retina. J. Neurosci. *22*, 2737–2747.
24. Laughlin, S.B. (1981). A simple coding procedure enhances a neuron's information capacity. Z. Naturforsch. [C] *36*, 910–912.
25. Laughlin, S.B. (1983). Matching coding to scenes to enhance efficiency. In Physical and Biological Processing of Images, O.J. Braddick and A. Sleigh, eds. (Berlin: Springer), pp. 42–52.
26. Rockhill, R.L., Daly, F.J., MacNeil, M.A., Brown, S.P., and Masland, R.H. (2002). The diversity of ganglion cells in a mammalian retina. J. Neurosci. *22*, 3831–3843.
27. Xu, Y., Dhingra, N.K., Smith, R.G., and Sterling, P. (2005). Sluggish and brisk ganglion cells detect contrast with similar sensitivity. J. Neurophysiol. *93*, 2388–2395.
28. Segev, R., Puchalla, J., and Berry, M.J., 2nd. (2006). Functional organization of ganglion cells in the salamander retina. J. Neurophysiol. *95*, 2277–2292.
29. Rieke, F., Bodnar, D.A., and Bialek, W. (1995). Naturalistic stimuli increase the rate and efficiency of information transmission by primary auditory afferents. Proc. Biol. Sci. *262*, 259–265.

30. Field, G.D., and Rieke, F. (2002). Nonlinear signal transfer from mouse rods to bipolar cells and implications for visual sensitivity. Neuron *34*, 773–785.
31. Attwell, D., and Gibb, A. (2005). Neuroenergetics and the kinetic design of excitatory synapses. Nat. Rev. Neurosci. *6*, 841–849.
32. Balasubramanian, V., Kimber, D., and Berry, M.J., 2nd. (2001). Metabolically efficient information processing. Neural Comput. *13*, 799–815.
33. Laughlin, S.B., de Ruyter van Steveninck, R.R., and Anderson, J.C. (1998). The metabolic cost of neural information. Nat. Neurosci. *1*, 36–41.
34. Levy, W.B., and Baxter, R.A. (1996). Energy efficient neural codes. Neural Comput. *8*, 531–543.
35. Attwell, D., and Laughlin, S.B. (2001). An energy budget for signaling in the grey matter of the brain. J. Cereb. Blood Flow Metab. *21*, 1133–1145.
36. Lennie, P. (2003). The cost of cortical computation. Curr. Biol. *13*, 493–497.
37. Sarpeshkar, R. (1998). Analog versus digital: Extrapolating from electronics to neurobiology. Neural Comput. *10*, 1601–1638.
38. Sterling, P. (2004). How retinal circuits optimize the transfer of visual information. In The Visual Neurosciences, L.M. Chalupa and J.S. Werner, eds. (Cambridge, MA: MIT Press), pp. 234–259.
39. Wassle, H., and Boycott, B.B. (1991). Functional architecture of the mammalian retina. Physiol. Rev. *71*, 447–480.
40. Brainard, D.H. (1997). The Psychophysics Toolbox. Spat. Vis. *10*, 433–436.
41. Pelli, D.G. (1997). The VideoToolbox software for visual psychophysics: Transforming numbers into movies. Spat. Vis. *10*, 437–442.
42. Van der Steen, J., and Collewijn, H. (1984). Ocular stability in the horizontal, frontal and sagittal planes in the rabbit. Exp. Brain Res. *56*, 263–274.
43. de Ruyter van Steveninck, R.R., Lewen, G.D., Strong, S.P., Koberle, R., and Bialek, W. (1997). Reproducibility and variability in neural spike trains. Science *275*, 1805–1808.
44. Strong, S.P., Koberle, R., de Ruyter van Steveninck, R.R., and Bialek, W. (1998). Entropy and Information in Neural Spike Trains. Phys. Rev. Lett. *80*, 197–200.

Supplemental Data
How *Much* the Eye Tells the Brain

Kristin Koch, Judith McLean, Ronen Segev, Michael A. Freed, Michael J. Berry II, Vijay Balasubramanian, and Peter Sterling

Supplemental References

S1. Koch, K., McLean, J., Berry, M., Sterling, P., Balasubramanian, V., and Freed, M.A. (2004). Efficiency of information transmission by retinal ganglion cells. Curr. Biol. *14*, 1523–1530.
S2. Wassle, H. (2004). Parallel processing in the mammalian retina. Nat. Rev. Neurosci. *5*, 747–757.
S3. Kier, C.K., Buchsbaum, G., and Sterling, P. (1995). How retinal microcircuits scale for ganglion cells of different size. J. Neurosci. *15*, 7673–7683.
S4. Vaney, D.I. (1994). Territorial organization of direction-selective ganglion cells in rabbit retina. J. Neurosci. *14*, 6301–6316.
S5. Yang, G., and Masland, R.H. (1994). Receptive fields and dendritic structure of directionally selective retinal ganglion cells. J. Neurosci. *14*, 5267–5280.

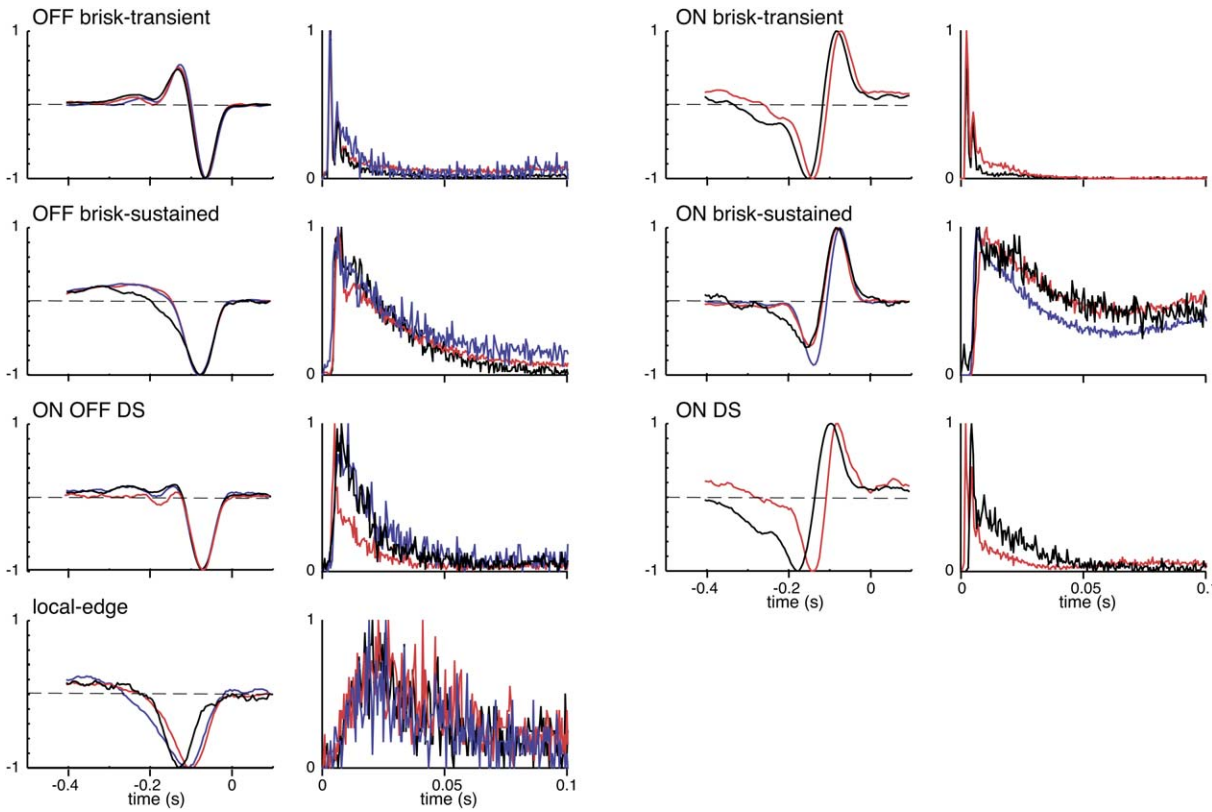

Figure S1. Cell Types Showed Distinct Spike-Triggered Averages and Autocorrelograms

For each type, the left panel shows superimposed spike-triggered averages to a flickering checkerboard stimulus (30 Hz) for 2–3 cells and the right shows superimposed autocorrelograms for the same cells. Cells in each panel were from one preparation (with the exception of ON brisk-transient cells which were taken from two different retinas). Local-edge cell types were confirmed by the cells' virtual silence to a spatially uniform full-field stimulus (<2 spikes $\cdot$ s^{-1} [S1]) and directionally selective types were confirmed by the cells' responses to moving gratings (direction-selective indices, i.e., $(R_{pref} - R_{null}) / (R_{pref} + R_{null}) > 0.7$). Of 107 cells, 18 belonged to the sluggish class yet could not be classified into distinct types.

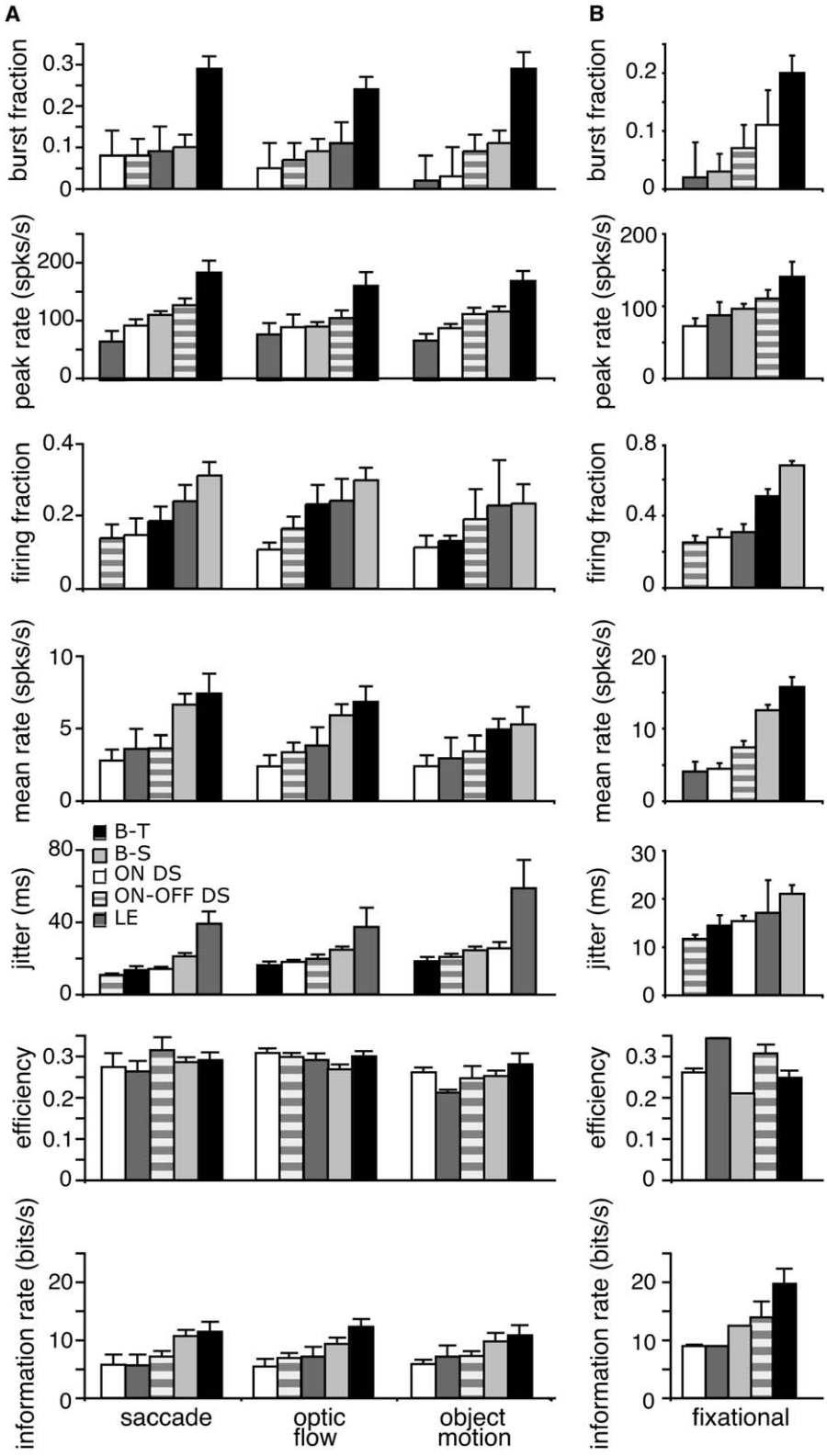

Figure S2. Spike Statistics and Information Rate Differed Between Cell Types More Than Between Scenes

Cells recorded on a multi-electrode array (A) or singly with a loose patch (B) are rank ordered by the average for each stimulus. The rank order is similar for all stimuli. The burst fraction was always highest for brisk-transient cells. The peak rate was always lowest for local-edge and highest for brisk-transient. Firing fraction was highest for brisk-sustained. Mean rate was always lower for direction-selective and local-edge than brisk-transient and brisk-sustained cells. Jitter was highest for local-edge and brisk-sustained cells. For all stimuli and cell types, efficiency was approximately 0.30. For all stimuli, direction-selective and local-edge types sent fewer bits $\cdot$ s^{-1} than brisk-transient. Error bars show standard error.

Table S1. Entropy Estimates Averaged over All Natural Stimuli

Cell Type	(Bits · s^{-1})	(Bits · Spk^{-1})	Information (% Capacity)	Total Entropy (% Capacity)	Noise Entropy (% Capacity)
Brisk-transient (n = 31)	13 ± 6	1.9 ± 0.5	29 ± 5%	85 ± 11%	56 ± 14%
ON brisk-transient (n = 5)	13 ± 4	1.7 ± 0.5	27 ± 5%	86 ± 16%	58 ± 20%
OFF brisk-transient (n = 26)	13 ± 6	1.9 ± 0.5	29 ± 5%	85 ± 10%	55 ± 13%
Brisk-sustained (n = 45)	10 ± 5	1.8 ± 0.6	27 ± 5%	89 ± 9%	62 ± 12%
ON brisk-sustained (n = 18)	9 ± 3	1.8 ± 0.5	27 ± 6%	88 ± 11%	61 ± 14%
OFF brisk-sustained (n = 27)	10 ± 6	1.9 ± 0.7	27 ± 5%	89 ± 8%	63 ± 11%
ON DS (n = 12)	6 ± 3	2.2 ± 0.6	28 ± 4%	90 ± 6%	62 ± 8%
ON-OFF DS (n = 25)	8 ± 4	2.2 ± 0.6	29 ± 6%	89 ± 10%	60 ± 12%
Local-edge (n = 14)	7 ± 3	2.1 ± 0.6	28 ± 5%	96 ± 5%	69 ± 7%

Fewer cells appear in Table S1 than Table 1 because data were not adequate to estimate noise entropy for some cells. All values are given as mean ± SD.

Table S2. Information down the Optic Nerve

Cell Type	Dendritic Area (mm^2)	Coverage Factor	Cell Density ($Cells/mm^2$)[a]	# of Cells	Bits · s^{-1} Per Array	Information Traffic (%)
Brisk-transient	0.20	3	30	6,000	78,000	9
Brisk-sustained	0.05	3	120	24,000	240,000	27
ON DS	0.13	1.5	36	7,000	42,000	5
ON-OFF DS	0.10	1.5	60	12,000	96,000	11
Local-edge	0.03	3	100	20,000	140,000	16
Sluggish (other)[b]				31,000	279,000	32
Total				100,000	875,000	

Cell numbers were estimated from dendritic-field area and coverage factor. For cell types with Gaussian-like receptive-field centers, the dendritic tips of one cell reach the somas of its nearest neighbors [S2]; therefore, if one assumes hexagonal packing, these cells' coverage factors roughly equal π. For cell types with flat-weighted receptive field centers (directionally-selective cells), coverage factors equal approximately 1.5 [S2–S5]. We divided each type's coverage factor by its dendritic field area (measured via dye injection) to yield cell density.

[a] Brisk-transient and brisk-sustained cells have two independent coverage factors, one for each polarity (ON and OFF). ON DS cells have three independent coverage factors, and ON-OFF DS cells have four, one for each of four cardinal directions. Accordingly, we multiplied brisk-transient and brisk-sustained cell density by 2, ON DS cell density by 3, and ON-OFF DS cell density by 4.

[b] Approximately 31,000 cells are of other sluggish cell types not represented in this study. We assigned these cells the average information rate for the sluggish cells we recorded but did not classify as to type.